
Figures and figure supplements

A subcellular map of the human kinome

Haitao Zhang et al

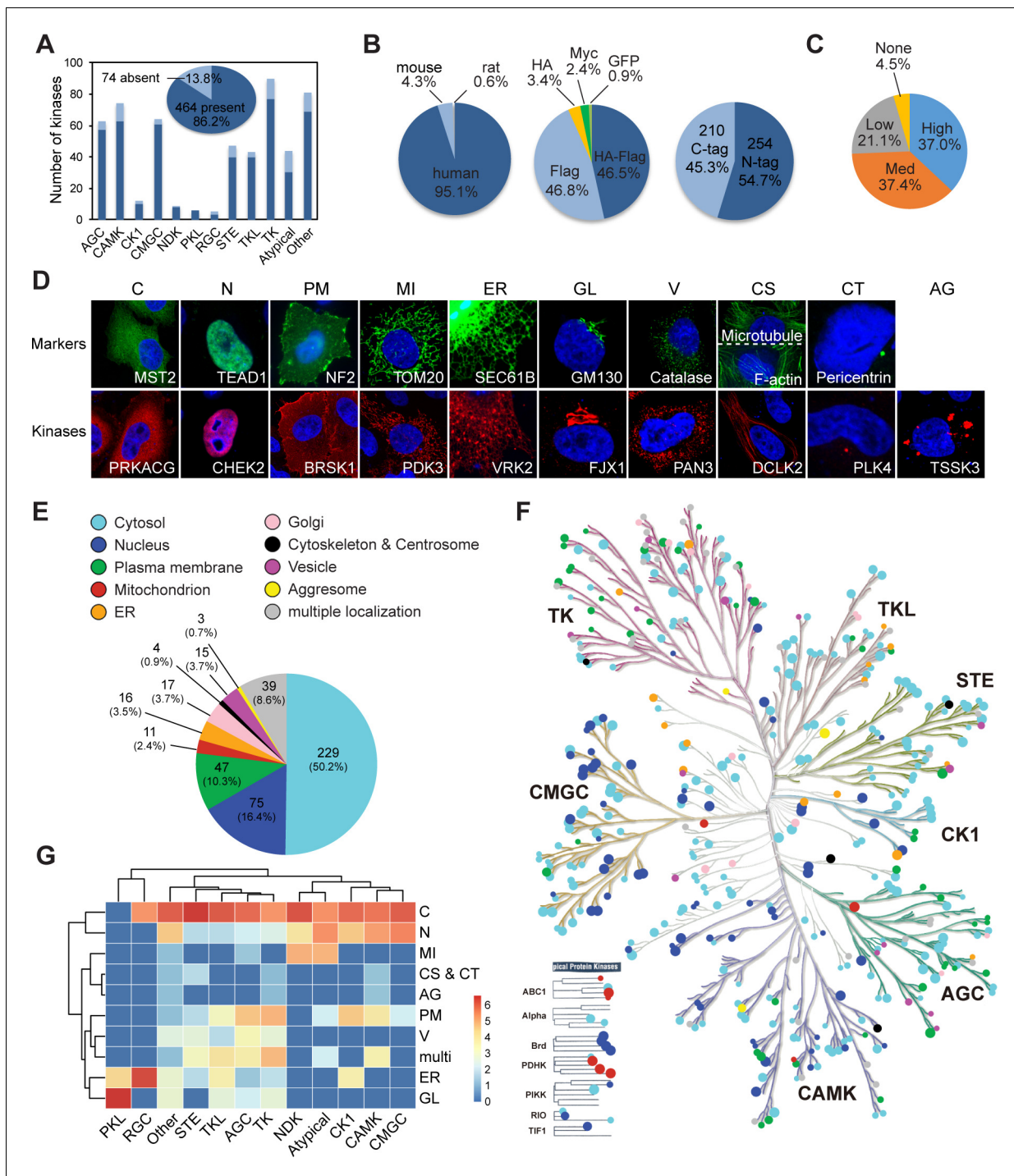


Figure 1. Mapping subcellular localizations of the kinome. (A) Coverage of the kinome (pie graph) and kinase families (bar graph) by the plasmid library. (B) Composition of the kinome library. Species origins (left), epitope tags (middle), and tag positions (right) were summarized. (C) Expression levels of kinase plasmids. HeLa cells were transfected and expression levels were determined by western blotting. (D) Ten cellular compartments with organelle markers (top) and representative kinases (bottom). SEC61B was visualized by GFP tag. TOM20, GM130, Catalase, microtubule, and pericentrin were stained by specific antibodies. F-actin was marked by phalloidin. Other proteins were transfected and stained for epitope tags. (E) Subcellular distribution of the kinome. (F) Kinome tree with localization information. Each dot represents a kinase. Color denotes compartment and size reflects localization score. (G) Family-enriched distributions for kinases. Kinase families were clustered by the ratio of localization to different compartments (**Figure 1—figure supplement 1**).

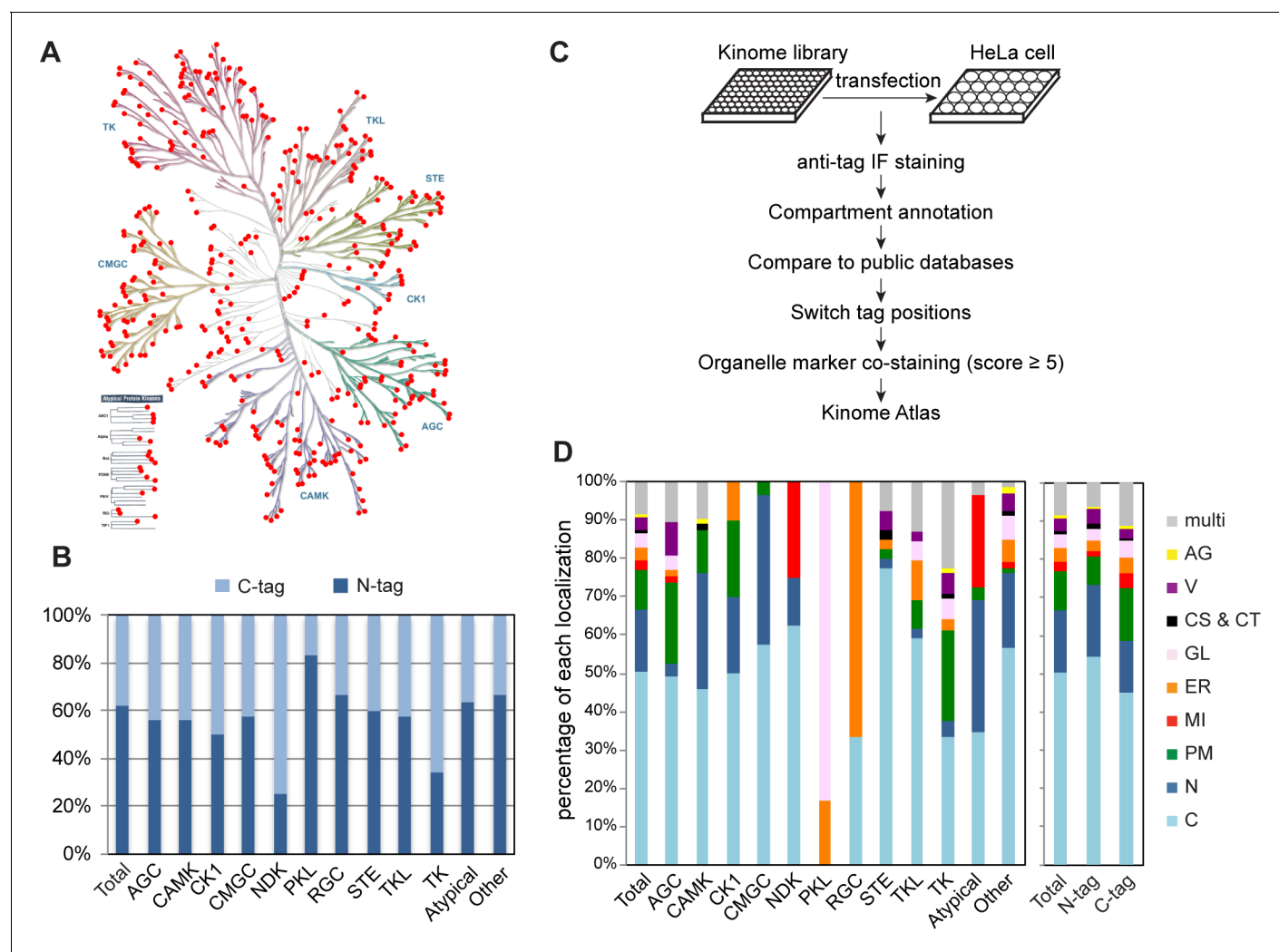


Figure 1—figure supplement 1. Mapping subcellular localizations of the kinome. (A) Distribution of the kinome plasmid library on the kinome tree. Each red dot represents a kinase in the library. (B) Ratio of N-terminal- and C-terminal-tagged kinases in each kinase family. (C) Flowchart of kinome subcellular localization mapping. (D) Distribution of 10 subcellular compartments in each kinase family (left panel) and in kinases with different tag positions (right panel).

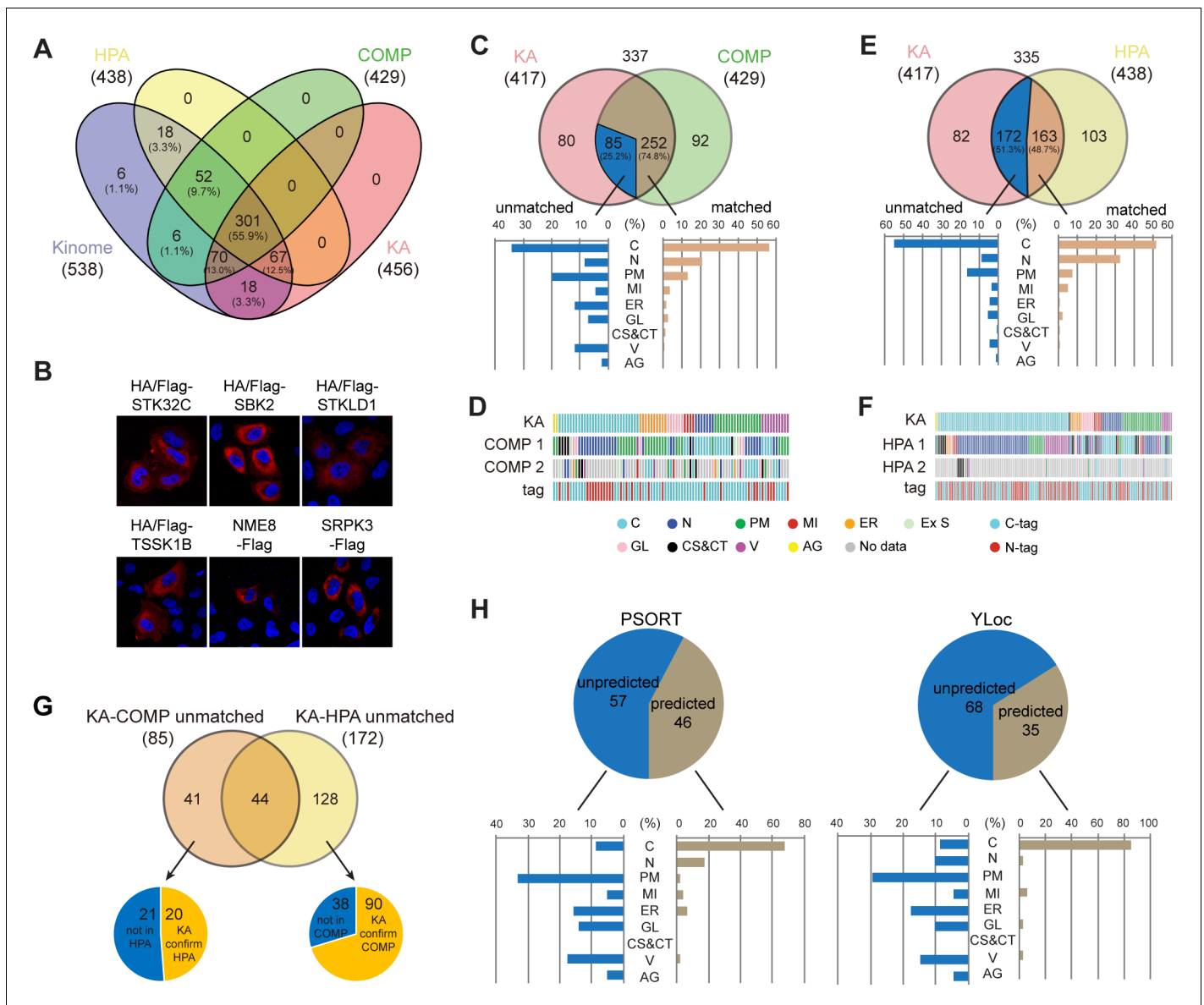


Figure 2. Kinome Atlas (KA) complements current databases for kinome localization. **(A)** Coverage of the kinome by COPARTMENTS, Human Protein Atlas (HPA), and KA in Venn diagram. **(B)** Subcellular localization of six kinases first annotated by KA. **(C, D)** Comparison of annotations in revised KA and high-confidence localizations in COMPARTMENTS. Distributions of matched and unmatched localizations are shown by bar graph. The heatmap demonstrates kinases (column) with color-coded localizations or position of epitope tag (row). Top two localizations in COMPARTMENTS are shown. **(E, F)** Comparison of annotations in HPA and KA. Analyses were similar to **(C, D)**. **(G)** KA provides unique kinase localizations different from databases. Kinases showing different annotations in KA-COMPARTMENTS or KA-HPA comparisons were further consolidated. **(H)** Prediction of KA-unique kinase localizations. Localizations of unique kinases in **(G)** were predicted by WoLF PSORT (left panel) or YLoc (right panel). Distribution of predicted or unpredicted kinases is shown by bar graph (**Figure 2—figure supplement 1**).

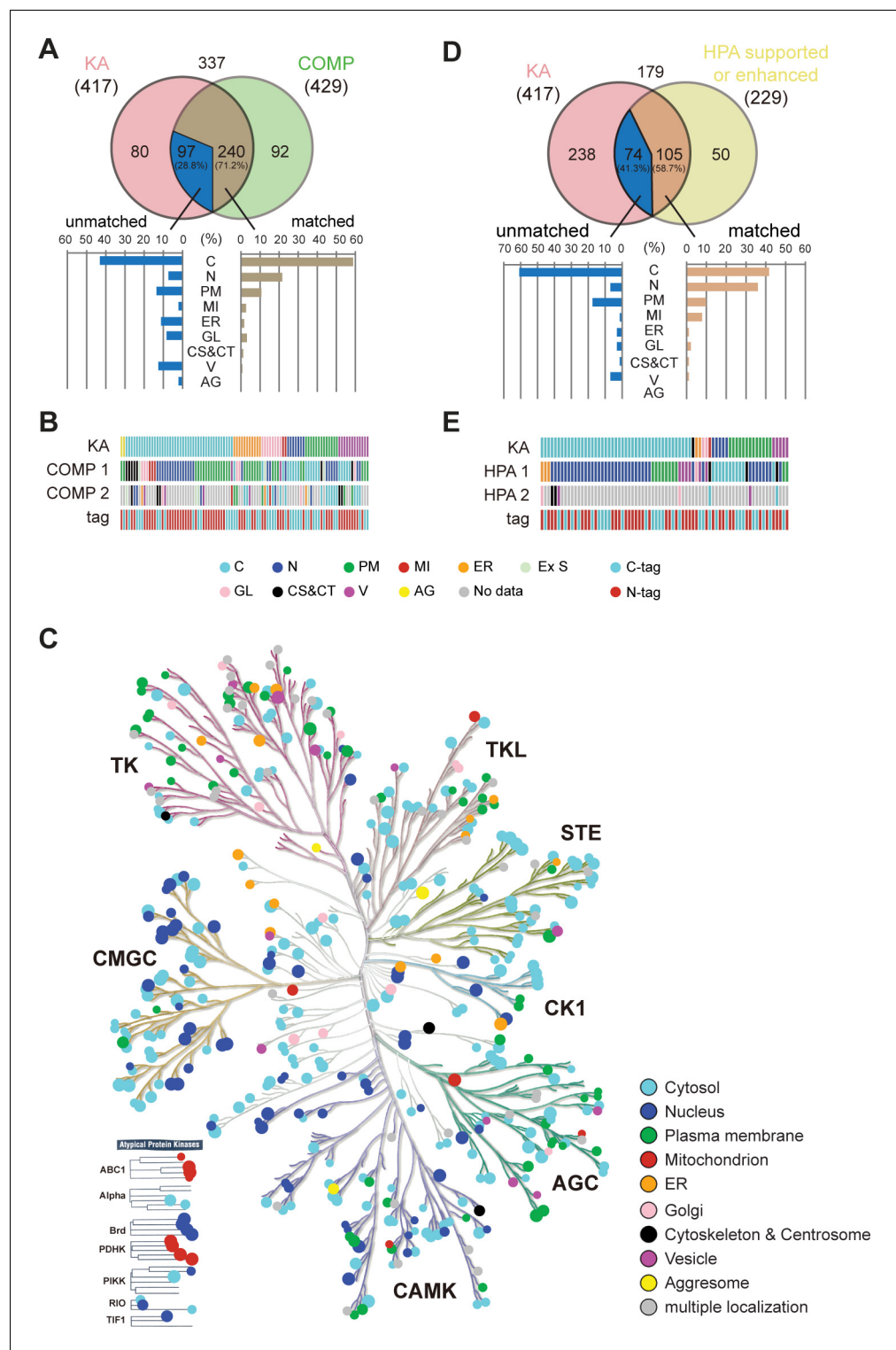


Figure 2—figure supplement 1. Kinome Atlas (KA) complements current databases for kinome localization. **(A)** Comparison of specific localizations in KA with high-confidence localizations in COMPARTMENTS. Distributions of matched and unmatched localizations are shown by bar graph. **(B)** The heatmap demonstrates kinases (column) with color-coded localizations or position of epitope tag (row). Top two localizations in COMPARTMENTS are shown. **(C)** Revised kinome tree with localization information. Each dot represents a kinase. Color denotes compartment and size reflects localization score. **(D, E)** Comparison of KA with 'enhanced' or 'supported' localizations in Human Protein Atlas (HPA). Analyses were similar to **(A, B)**.

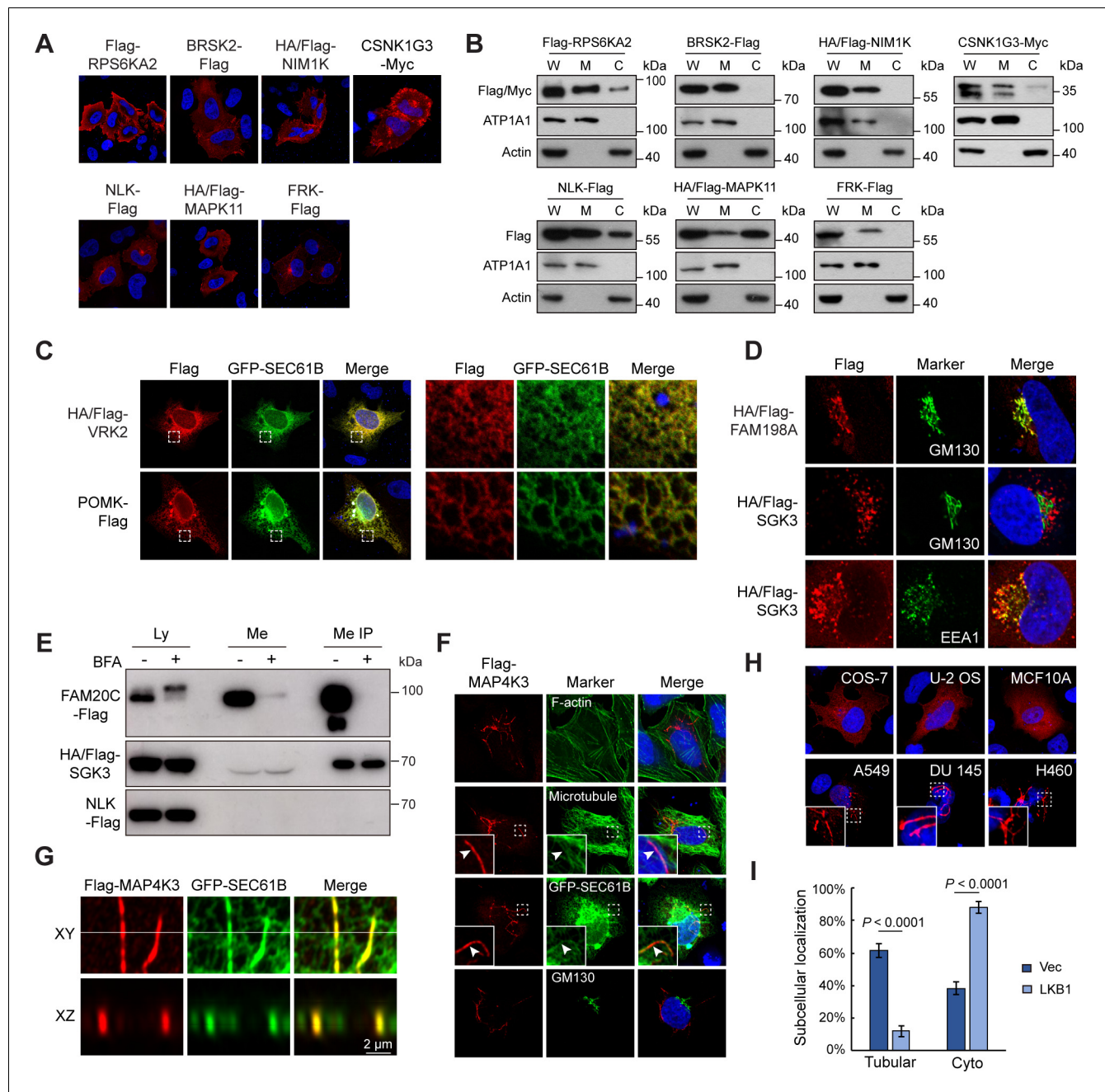


Figure 3. Kinome Atlas (KA) identified unknown localizations for kinases. (A, B) New plasma membrane-localized kinases identified by KA. Original mapping data (A) and confirmation by cellular fractionation (B). W: whole cell lysate; M: membrane; C: cytosol. Equal loading was achieved by normalizing to the same number of cells. (C) Confirmation of endoplasmic reticulum (ER)-localized kinases. HeLa cells were co-transfected with kinase and GFP-SEC61B. VRK2 was used as a positive control of ER protein. Squared areas were enlarged on the right. (D) Confirmation of SGK3 localization in transfected HeLa cells. (E) SGK3 was secreted to culture medium. HEK293T cells were transfected and brefeldin A (BFA) (0.5 μ g/ml) treated for 24 hr as indicated. Both culture medium and cell lysates were collected. Medium was further immunoprecipitated by anti-Flag antibody. Loading was normalized by the number of input cells, and IP samples were loaded at 5 \times of input. (F) MAP4K3 colocalizes with microtubule and ER in HeLa cells. Arrowheads indicate colocalization. (G) MAP4K3 colocalizes with SEC61B as captured by Zeiss Airyscan high-resolution microscopy. (H) Cell-type-dependent localization of MAP4K3. Indicated cells were transfected with Flag-MAP4K3 and stained by anti-Flag antibody. (I) LKB1 inhibits tubule-like localization of MAP4K3. Control and LKB1-expressing H460 cells were transfected with Flag-MAP4K3 and were stained by anti-Flag antibody. Cells with different localization patterns were quantified. Data was represented as mean \pm SD; $n = 3$ independent experiments, two-tailed Student's t test; $n = 100$ cells were analyzed in each experiment (Figure 3—figure supplement 1).

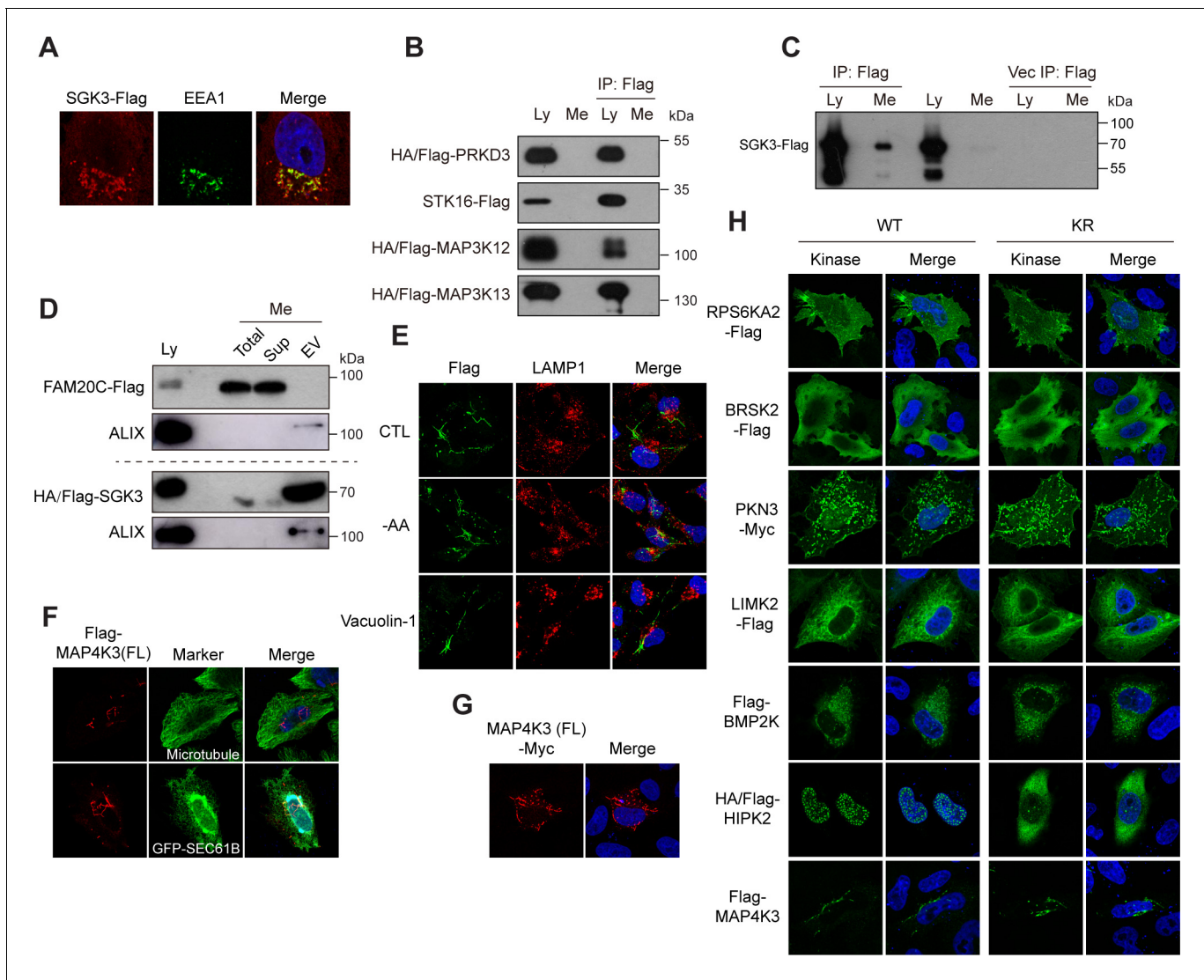


Figure 3—figure supplement 1. Kinome Atlas (KA) identified unknown localizations for kinases. (A) C-terminal tagged SGK3 colocalizes with EEA1 in HeLa cells. (B) PRKD3, STK16, MAP3K12, and MAP3K13 are not secreted. HEK293T cells were transfected. Both culture medium and cell lysates were collected and immunoprecipitated by anti-Flag M2 resin. Loading was normalized by the number of input cells, and IP samples were loaded at 5× of input. (C) C-terminal tagged SGK3 was secreted to culture medium. Experiments were similar to (B). (D) Presence of SGK3 in exosomes. Culture mediums were ultracentrifuged, and fractions were examined by western blotting. Loading was normalized by the number of input cells, and EV fractions were loaded at 5× of input. ALIX is a marker of exosome. (E) MAP4K3 does not colocalize with lysosome. HeLa cells were transfected with Flag-MAP4K3. Cells were starved in Hanks' Balanced Salt Solution containing 10% dialyzed FBS and 4.5 g/L glucose for 6 hr or treated with 200 nM vacuolin-1 for 1.5 hr. Cells were stained with anti-Flag and anti-LAMP1 antibodies. (F) N-terminal tagged full-length MAP4K3 exhibits tubule-like structures colocalizing with microtubule and endoplasmic reticulum (ER) in HeLa cells. (G) C-terminal tagged full-length MAP4K3 exhibits tubule-like structures in HeLa cells. (H) Subcellular localization of inactive kinases. Wildtype kinases and kinase inactive mutants (KR) were transfected into HeLa cells. Cells were then fixed and stained.

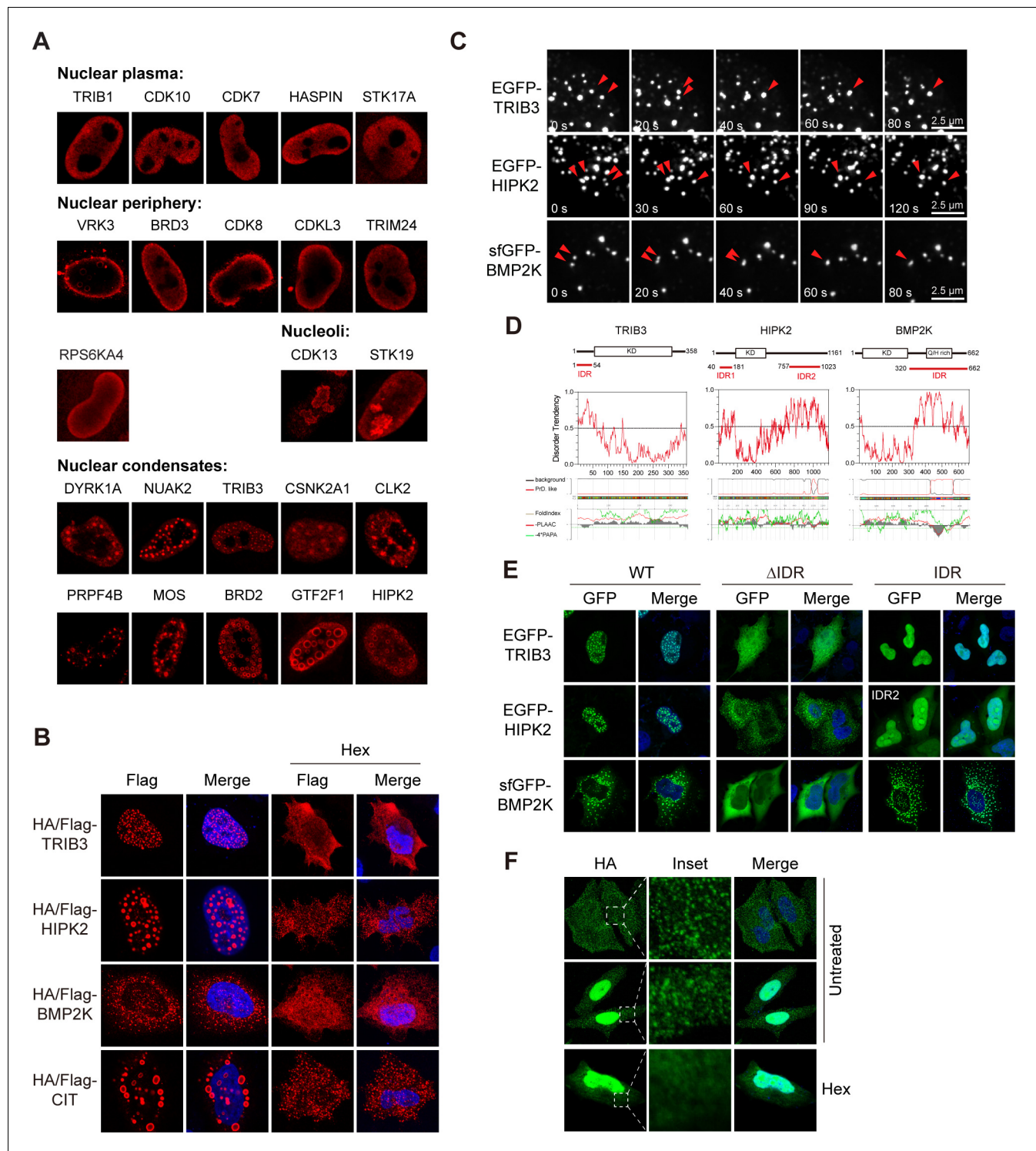


Figure 4. Phase separation assemblies kinase condensates. (A) Sub-nuclear patterns of kinases in Kinome Atlas (KA). (B) Hex disrupts puncta localization of kinases. Transfected HeLa cells were treated with 10% 1,6-hexanediol (Hex) for 1 min as indicated. Cells were then fixed and stained. (C) Fusion of kinase puncta in live cells. HeLa cells expressing GFP-tagged kinases were examined by time-lapse microscopy. Fusion events were indicated by arrowheads. (D) Sequence analysis identified intrinsically disordered regions (IDRs) in kinases. Domain organizations were illustrated in scale. KD: kinase domain. Disorder tendency was predicted by IUPred2A. Prion-like regions and fold index were predicted by PLAAC. (E) Deletion of IDR impairs puncta localization. Wildtype or mutants with GFP tag were expressed and visualized in HeLa cells. For HIPK2, both IDRs were deleted in Δ IDR. (F) Puncta formed by endogenous BMP2K in HeLa cells. BMP2K 3xHA tag knock-in HeLa cells were treated with 10% Hex for 1 min as indicated. Cells were then fixed and stained (**Figure 4—figure supplement 1**).

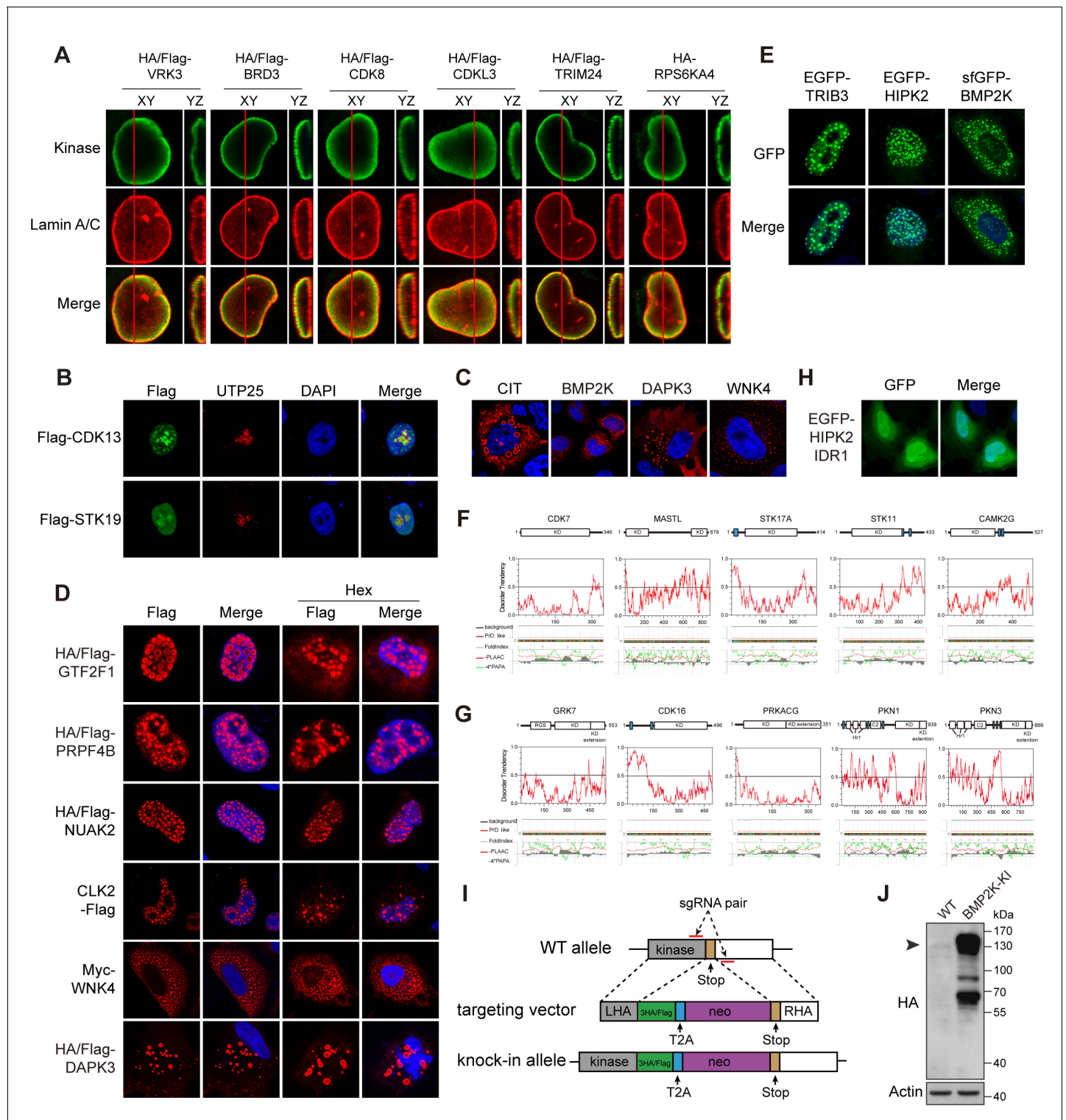


Figure 4—figure supplement 1. Phase separation assemblies kinase condensates. (A) Nuclear peripheral kinases visualized by Airyscan high-resolution microscopy. Transfected HeLa cells were stained with anti-HA for the kinase and anti-Lamin A/C for nuclear envelope. (B) Confirmation of CDK13 and STK19 in nucleoli. HeLa cells were transfected and stained by anti-Flag and anti-UTP25 antibodies. (C) Cytoplasmic puncta formed by kinases. (D) Hex-resistant puncta formed by kinases. Transfected HeLa cells were treated with 10% Hex for 1 min as indicated. Cells were then fixed and stained. (E) GFP tag did not affect puncta localization of examined kinases. GFP-tagged kinases were expressed and imaged in HeLa cells. (F, G) Sequence analysis of randomly selected nuclear (F) and cytosolic (G) kinases with even distribution. Domain organizations were illustrated in scale. KD: kinase domain. Blue bars represent low complexity domains. Disorder tendency was predicted by IUPred2A. Prion-like regions and fold index were predicted by PLAAC. (H) Figure 4—figure supplement 1 continued on next page

Figure 4—figure supplement 1 continued

Subcellular localization of HIPK2 intrinsically disordered region (IDR)1. HIPK2 IDR1 with GFP tag was expressed and visualized in HeLa cells. (I) Knock-in of epitope tags with CRISPR/Cas9 technology. L/RHA: left/right homologous arm. (J) Confirmation of BMP2K knock-in cells by western blotting. Arrowhead denotes BMP2K in predicted molecular weight.

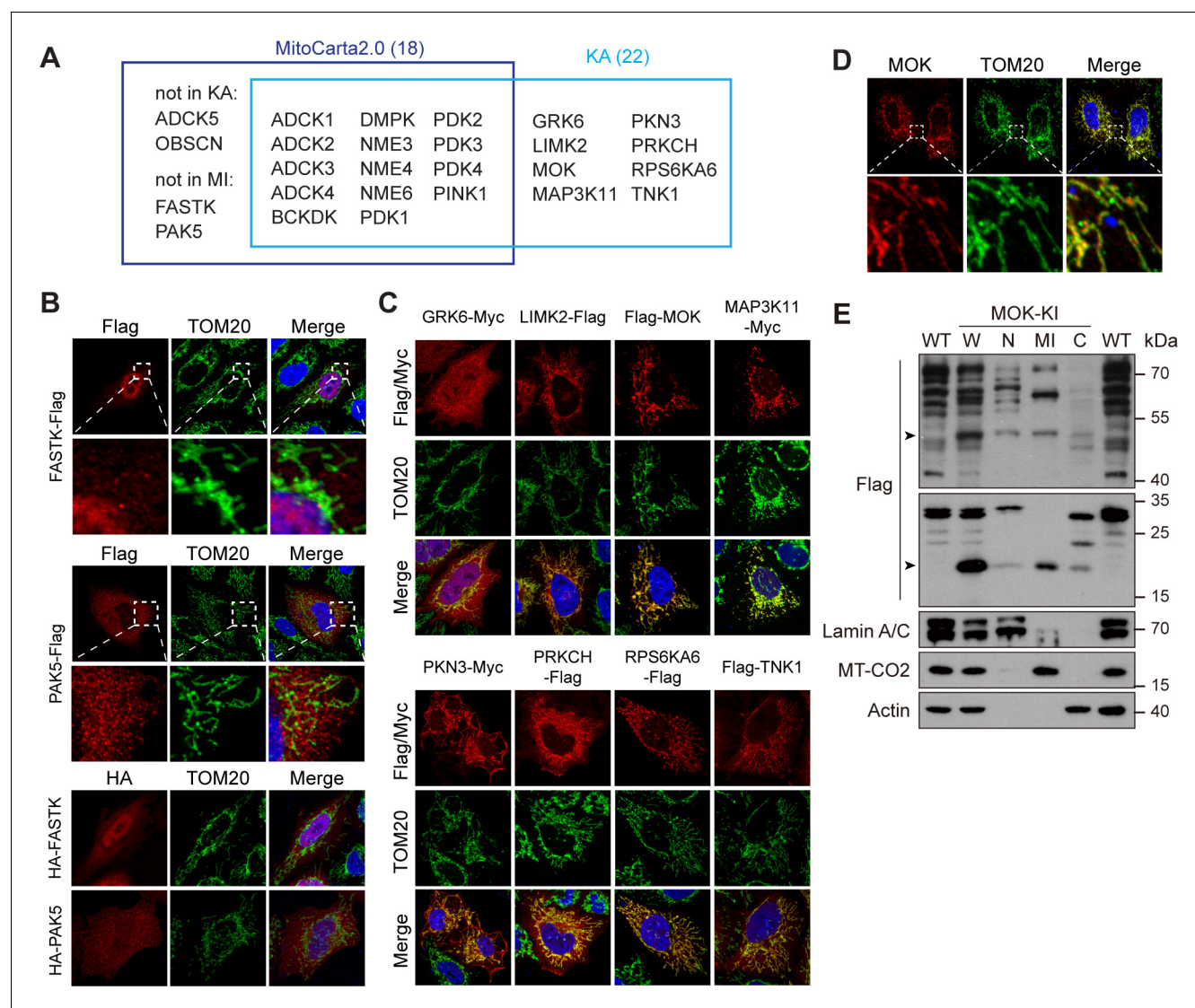


Figure 5. Kinome Atlas (KA) identified novel mitochondrial kinases. **(A)** Comparison of MitoCarta2.0 and KA. **(B)** FASTK and PAK5 are not mitochondrial. N- and C-terminal tagged kinases were expressed in HeLa cells and stained. **(C)** Mitochondrial kinases identified by KA. Experiments are similar to **(B)**. **(D)** Overexpressed tagless MOK localized to mitochondria. Transfected HeLa cells were fixed and stained with anti-MOK antibody. **(E)** Endogenous MOK was present in mitochondria. MOK 3x Flag knock-in HeLa cells were fractionated and examined by western blotting. W: whole cell lysate; N: nucleus; MI: mitochondria; C: cytosol. Lamin A/C, MT-CO2, and Actin are nuclear, mitochondrial, and cytosolic markers, respectively. Equal loading was achieved by normalizing to the same number of cells. Arrowheads indicate MOK (**Figure 5—figure supplement 1**).

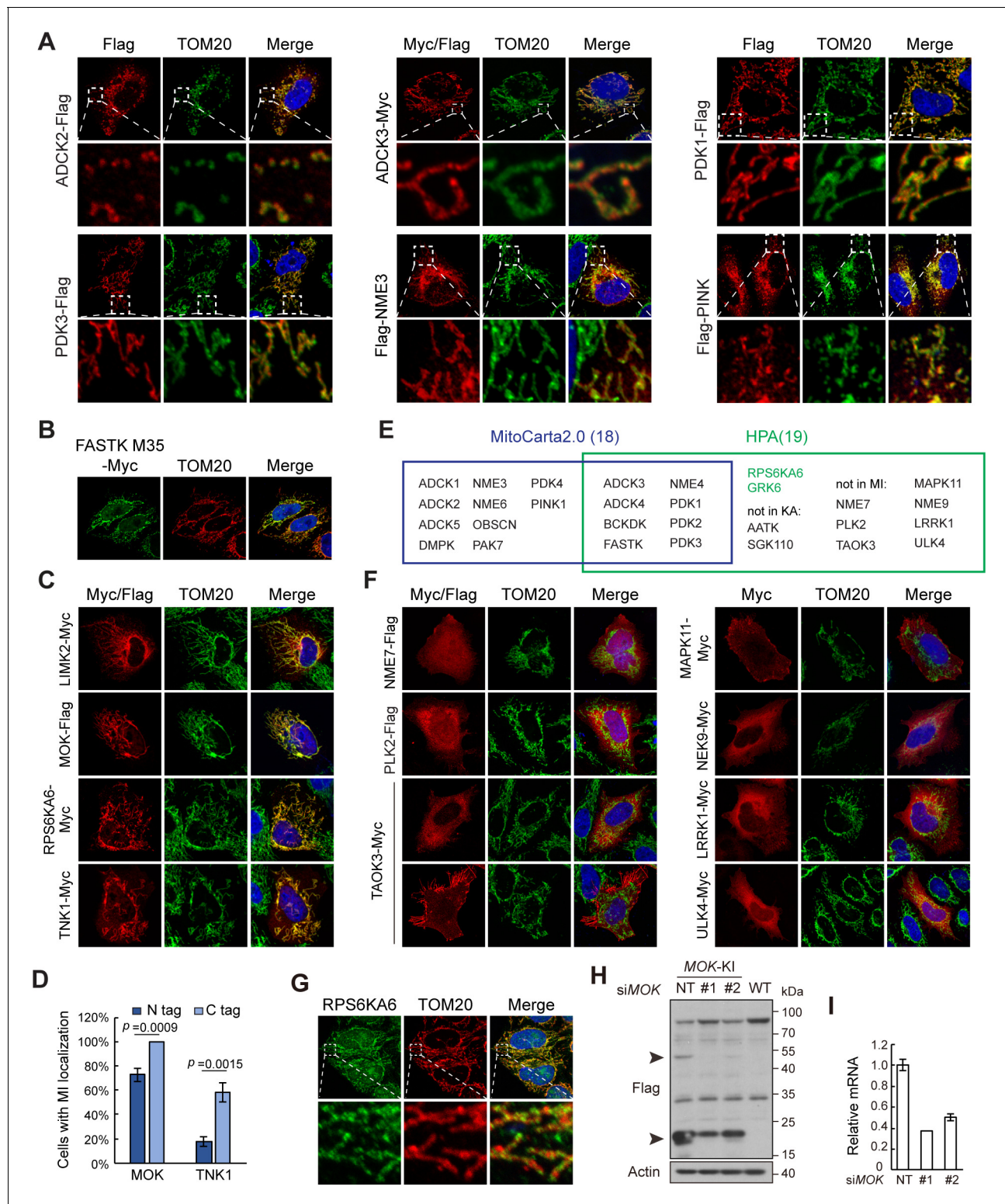


Figure 5—figure supplement 1. Kinome Atlas (KA) identified novel mitochondrial kinases. (A) Confirmation of mitochondrial kinases by co-staining with TOM20. (B) N-terminal truncated isoform of FASTK exhibited mitochondrial localization. FASTK-M35 was transfected in HeLa cells and stained with anti-Myc antibody. (C) Confirmation of mitochondrial kinases in MCF10A cells. C-terminal-tagged kinases were expressed in MCF10A cells and stained. (D) Effect of tag position on MOK and TNK1 mitochondrial localization. MOK and TNK1 tagged on either end were expressed in HeLa cells, and 100 cells in random views were quantified for mitochondrial localization. Data is represented as mean \pm SD; $n = 3$ independent experiments, two-tailed Student's t test. (E) Comparison of mitochondrial kinases in MitoCarta2.0 and Human Protein Atlas (HPA). Kinases only in HPA and confirmed by KA

Figure 5—figure supplement 1 continued on next page

Figure 5—figure supplement 1 continued

were labeled in green. (F) Kinases were tagged on the C-terminal, transfected, and stained in HeLa cells. (G) Endogenous RPS6KA6 of HeLa cells was stained by a specific antibody. (H) MOK 3x Flag knock-in HeLa cells were transfected with non-targeting or specific siRNAs, and cell lysates were examined by western blotting. (I) MOK siRNA knockdown efficiency as determined by quantitative RT-PCR.

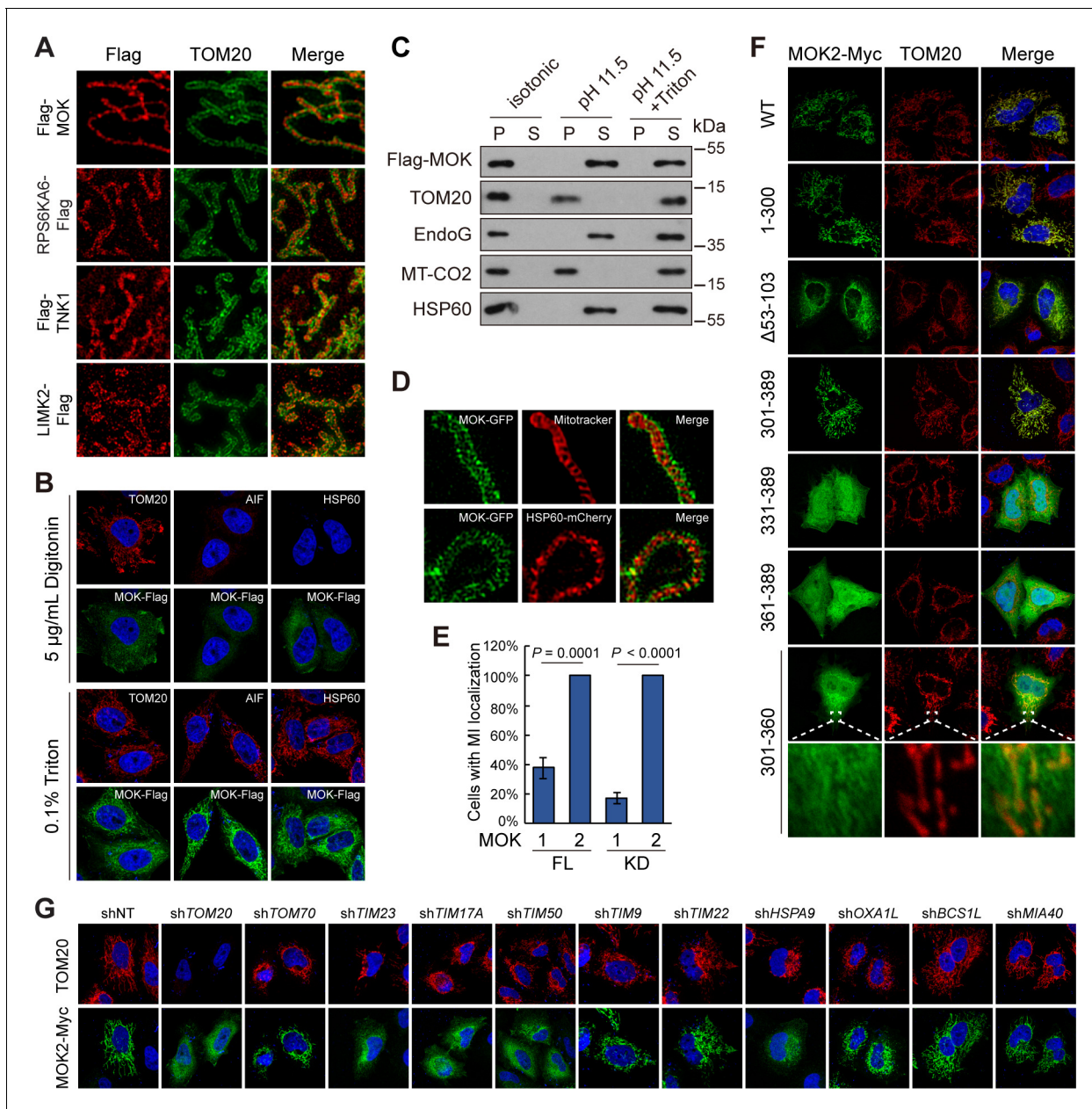


Figure 6. MOK is a mitochondrial intermembrane space (IMS)-localized protein. (A) Sub-mitochondrial localizations of new mitochondrial kinases. Transfected HeLa cells were stained and imaged by 3D structured illumination microscopy (3D-SIM). (B) MOK2 is imported into mitochondria. Transfected HeLa cells were fixed and permeabilized with digitonin or Triton X-100 before staining. (C) MOK is not a mitochondrial membrane protein. Mitochondria purified from transfected HeLa cells were incubated in indicated buffers, and then centrifuged. Supernatants (S) and pellets (P) were analyzed by western blotting. Equal loading was achieved by normalizing to the same number of cells. (D) MOK is an IMS protein. COS-7 cells transfected with MOK2-GFP were imaged by Hessian SIM. MitoTracker Red marked inner membrane (IMM) and co-transfected HSP60-mCherry marked matrix. (E) MOK2 has better mitochondrial localization than MOK1. HeLa cells were transfected with full-length (FL) or kinase domain (KD) of MOK1 and MOK2. Cells with mitochondrial MOK were quantified. Data is represented as mean \pm SD; $n = 3$ independent experiments, two-tailed Student's t test; $n = 100$ cells were analyzed in each experiment. (F) Mitochondrial localization of MOK mutants. Transfected HeLa cells were stained with anti-Myc and anti-TOM20 antibodies. (G) TOM20-TIM23 complex is required for mitochondrial importing of MOK. HeLa cells expressing specific shRNAs were transfected with MOK2-Myc and stained (**Figure 6—figure supplement 1**).

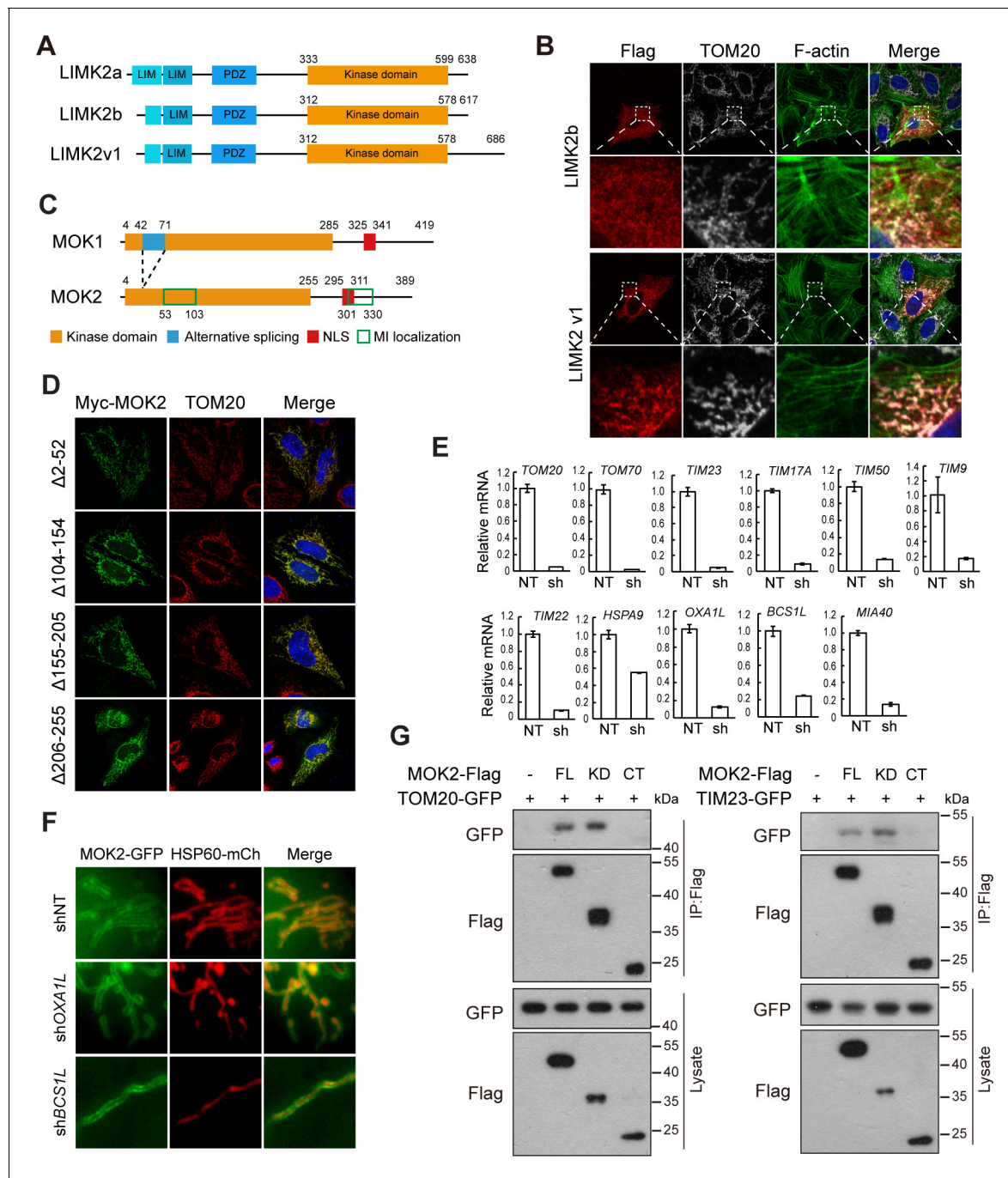


Figure 6—figure supplement 1. MOK is a mitochondrial intermembrane space (IMS)-localized protein. (A) Domain organization of LIMK2 isoforms. (B) Subcellular localization of LIMK2 isoforms. HeLa cells transfected with LIMK2 isoforms were stained with anti-Flag and anti-TOM20 antibodies. F-actin was marked by phalloidin staining. (C) Domain organization of MOK1 and MOK2. NLS: nuclear localization signal. Sequences responsible for mitochondrial localization are marked by green boxes. (D) Subcellular localization of MOK mutants. Transfected HeLa cells were stained with anti-Myc and anti-TOM20 antibodies. (E) Knockdown efficiency of shRNAs were determined by quantitative RT-PCR. NT: non-targeting control. Data is represented as mean \pm SD from three technical repeats. (F) Knockdown of *OXA1L* and *BCS1L* did not affect MOK2 sub-mitochondrial localization. HeLa cells expressing indicated shRNAs were transfected with MOK2-GFP and HSP60-mCherry. (G) MOK2 interacts with TOM20 and TIM23. HEK293T cells were transfected and lysed for immunoprecipitation by anti-Flag resin. FL: full-length; KD: kinase domain; CT: C-terminus.

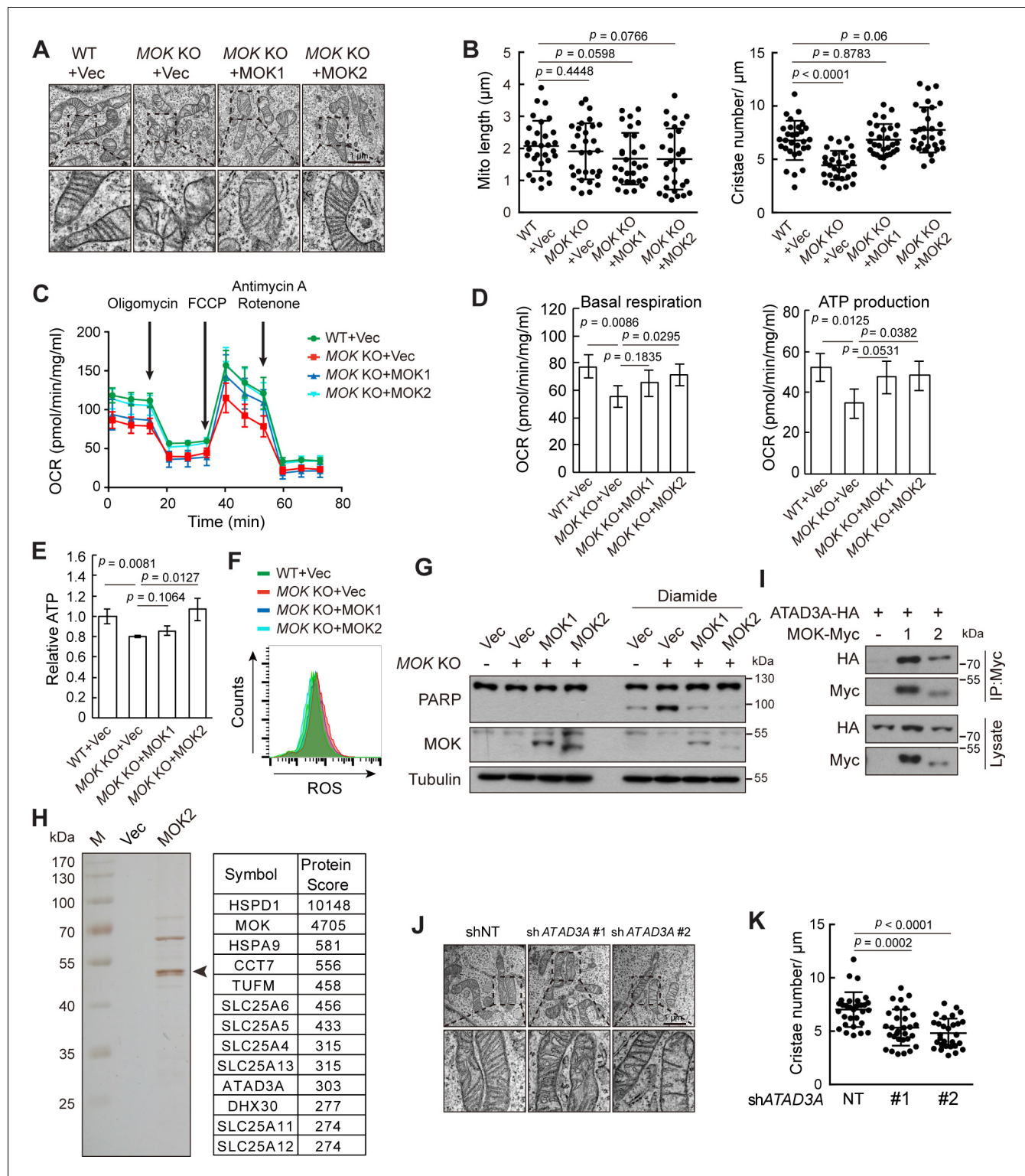


Figure 7. Knockout (KO) of MOK impairs mitochondrial structure and functions. (A, B) MOK KO reduced mitochondria cristae. Indicated A375 cells were examined by electron microscopy (A). The length and cristae number of mitochondria ($n = 30$) were quantified (B). (C, D) MOK KO impairs mitochondrial respiration. Cells sequentially exposed to mitochondrial inhibitors were analyzed on a Seahorse Analyzer. Oxygen consumption rate (OCR) was measured and normalized to protein concentration (C). Respiratory parameters were calculated from OCR data as described in the Materials and methods section (D). Data is representative and represented as mean \pm SD, $n = 3$, two-tailed Student's t test. (E) MOK KO reduced cellular ATP level. Data is representative and represented as mean \pm SD, $n = 3$, two-tailed Student's t test. (F) MOK KO increased cellular reactive oxygen species (ROS) level. Data is representative and represented as mean \pm SD, $n = 3$, two-tailed Student's t test. (G) MOK KO cells show increased sensitivity to Diamide. (H) MOK KO cells show increased sensitivity to MOK2. (I) MOK KO cells show increased sensitivity to Diamide. (J) sh ATAD3A cells show increased sensitivity to Diamide. (K) sh ATAD3A cells show increased sensitivity to Diamide. Figure 7 continued on next page

Figure 7 continued

oxygen species (ROS) level. Cells were stained with CM-H2DCFDA followed by flow cytometry. (G) MOK KO promoted apoptosis in response to oxidative stress. Indicated A375 cells were treated with 200 nM diamide for 20 hr, and cell lysates were analyzed by western blotting. (H) TAP identified MOK2 interacting proteins in mitochondria. MOK2-Flag-SBP was expressed in MCF10A cells, purified, and analyzed by silver staining after electrophoresis (left). Arrowhead denotes MOK. Top hits from mass spectrometry are shown (right). (I) MOK interacts with ATAD3A. HEK293T cells were transfected and cell lysates were immunoprecipitated with anti-Myc antibody. (J, K) Knockdown of ATAD3A reduced mitochondrial cristae number. Experiments were similar to these in (A, B). Data is representative and represented as mean \pm SD, $n = 30$, two-tailed Student's t test (**Figure 7—figure supplement 1**).

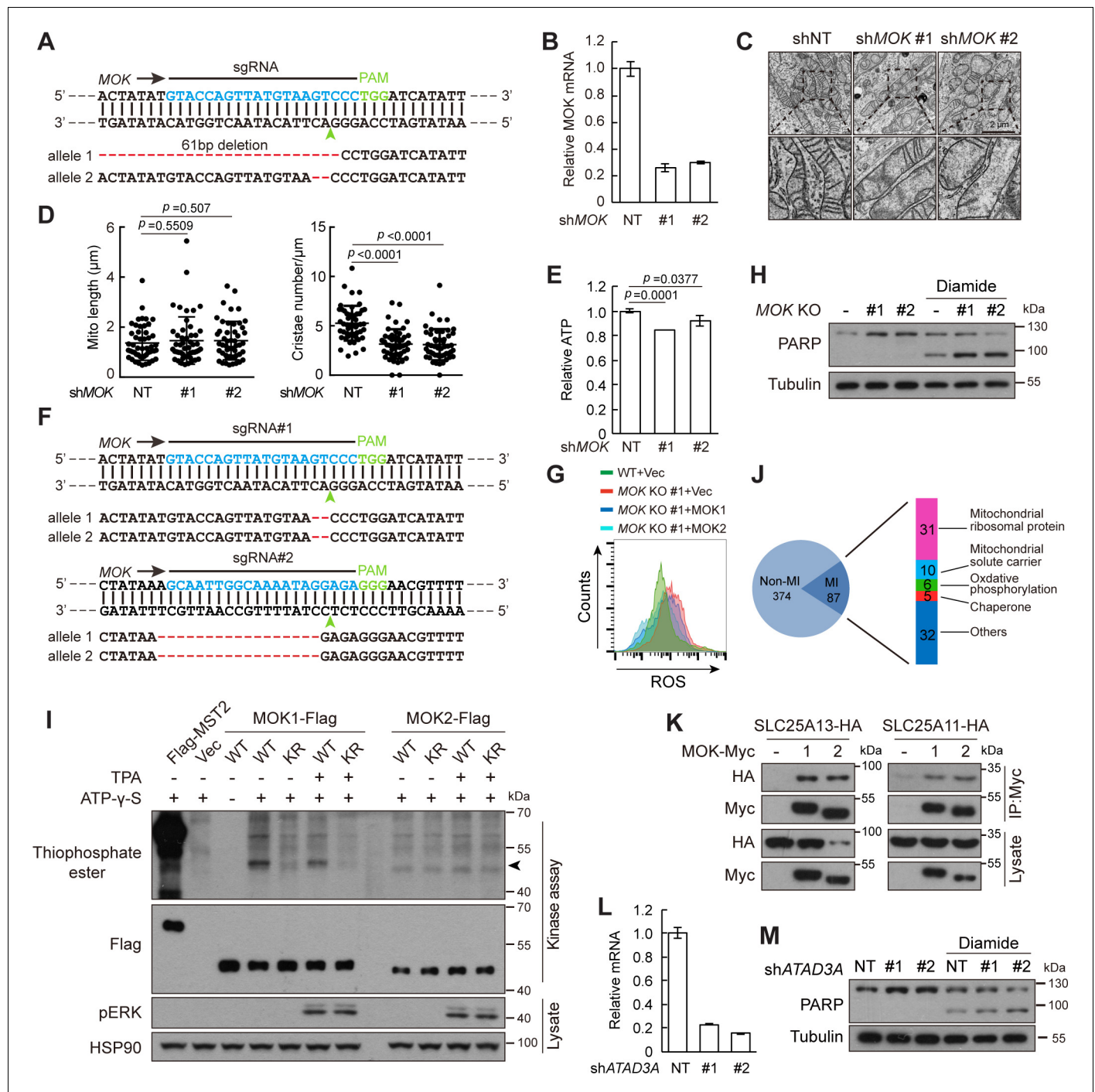


Figure 7—figure supplement 1. Knockout of MOK impairs mitochondrial structure and functions. (A) Confirmation of MOK knockout in A375 cells by genomic DNA sequencing. Indels are labeled in red. Arrowhead indicates predicted Cas9 cutting site. (B) MOK knockdown efficiency in Caki-1 cells as determined by quantitative RT-PCR. (C, D) Knockdown of MOK reduced mitochondria cristae in Caki-1 cells. The length and cristae number of mitochondria (n = 50) were quantified. Data is represented as mean ± SD, two-tailed Student's t test. (E) Knockdown of MOK in Caki-1 cells reduced cellular ATP level. Data is represented as mean ± SD. n = 3 repeats, two-tailed Student's t test. (F) Confirmation of MOK knockout in MCF10A cells by genomic DNA sequencing. (G) Knockout of MOK increased cellular reactive oxygen species (ROS) level. Cells were treated with 150 mM H₂O₂ for 15 min and analyzed by flow cytometry. (H) Knockout of MOK promoted apoptosis in response to oxidative stress. Indicated cells were treated with 200 nM diamide for 20 hr, and cell lysates were analyzed by western blotting. (I) MOK2 lacks kinase activity. MOK was immunoprecipitated from transfected HEK293T cells and subjected to in vitro kinase activity assay. Phosphorylation was detected by anti-thiophosphate-ester antibody. Arrowhead denotes MOK autophosphorylation. To activate MAPK signaling, cells were treated with 100 ng/ml tetradecanoyl phorbol acetate (TPA) for 30 min. Flag-MST2

Figure 7—figure supplement 1 continued on next page

Figure 7—figure supplement 1 continued

was used as a positive control. KR denotes a kinase inactive mutant generated by mutating the ATP binding Lys to Arg. (J) Distribution of MOK-interacting proteins identified from TAP purification. (K) MOK interacts with SLC25A13 and SLC25A11. HEK293T cells were transfected and cell lysates were immunoprecipitated by anti-Myc antibody. (L) ATAD3A knockdown efficiency in A375 cells as determined by quantitative RT-PCR. (M) Knockdown of ATAD3A did not promote A375 apoptosis in response to oxidative stress. Indicated cells were treated with 200 nM diamide for 20 hr, and cell lysates were analyzed by western blotting.